Enhancement of Standard ECGs by a New Method for Multi-Cycle Superimposition and Summation

Aharon Frimerman MD, Simcha Meisel MD, Avraham Shotan MD and David S. Blondheim MD

Department of Cardiology, Hillel Yaffe Medical Center, Hadera, affiliated with Rappaport Faculty of Medicine, Technion–Israel Institute of Technology, Haifa, Israel

ABSTRACT: **Background:** Since the introduction of the electrocardiogram (ECG) in 1902, the fundamentals of ECG data acquisition, display, and interpretation in the clinical arena have not changed much.

Objectives: To present a new method to enhance and improve acquisition, analysis, and display of the standard ECG.

Methods: We performed ECG enhancement by superimposition and summation of multiple standard ECG cycles of each lead, by temporal alignment to peak R wave and voltage alignment to an improved baseline, at the T-P segment.

Results: We enhanced ECG recordings of 504 patients who underwent coronary angiograms for routine indications. Several new ECG features were noted on the enhanced recordings. Examination of a subgroup of 152 patients with a normal rest 12-lead ECG led to the discovery of a new observation, which may help to distinguish between patients with and without coronary artery disease (CAD): namely, a spontaneous cycle-to-cycle voltage spread (VS) at the S-T interval, normalized to VS at the T-P interval. The mean normalized VS was significantly greater in those with CAD (n=61, 40%) than without (n=91, 60%), 5.61 ± 3.79 vs. 4.01 ± 2.1 ($P < 0.05$).

Conclusions: Our novel method of multiple ECG-cycle superimposition enhances the ECG display and improves detection of subtle electrical abnormalities, thus facilitating the standard rest ECG diagnostic power. We describe, for the first time, voltage spread at the S-T interval, an observed phenomenon that can help detect CAD among individuals with normal rest 12-lead ECG.

IMAJ 2018; 20: 14–19

KEY WORDS: electrocardiogram (ECG), signal enhancement, coronary angiogram, coronary artery disease, voltage spread

Since 1902, when Willem Einthoven introduced the electrocardiogram (ECG), this method has become an established medical diagnostic tool [1]. Several modifications of the ECG were introduced over the years but basically the fundamentals of ECG data acquisition, and its display and interpretation in the clinical arena, have not changed much since Einthoven's time.

Disclosure: Dr. Aharon Frimerman provides complementary consultation to BSA, Tel Aviv, Israel

We designed a new system that combines a slightly modified machine with novel software for enhancement, analysis, and display of ECGs using contemporary computing technology.

The purpose of the current study was to describe our novel method for ECG enhancement, and to demonstrate the virtues of the enhanced ECG display. Our investigation led to the observation of new parameters that were derived from the improved ECGs. We tested the potential of these parameters to improve the limited diagnostic power of standard rest 12-lead ECG for identification of patients with significant underlying CAD [2]. Our new technique enhances the ECG signal by using a novel processing method for summation and superimposition (not averaging) of multiple ECG complexes of each lead. The method reveals fine waves that are undetected or can be missed in standard ECG displays.

PATIENTS AND METHODS

ECG ACQUISITION DEVICE

To improve sampling duration and accuracy of a standard ECG acquisition device, we selected a 3-channel machine (Nihon Kohden ECG-6511; Nihon Kohden, Tokyo, Japan), which simultaneously acquired 3 minutes of synchronized multiple leads. To simplify our analysis we took two simultaneous acquisitions: leads I, II, III, representing the limb leads; and subsequently leads V2, V4, V6, representing the chest leads. We developed dedicated software to capture and perform measurements, digital operations, and display and to store the data on the three synchronized channels. Standard ECGs were taken for comparison at a paper speed of 25 mm/s, calibration of 10 mm/mV, and regular filtering.

MULTIPLE ECG CYCLE SUMMATION FOR SIGNAL ENHANCEMENT

To enhance the ECG signal, multiple cycles (about 200) from each lead were superimposed to obtain a single improved graphical display of the complex. To acquire a consistent superimposition, temporal and voltage (i.e., baseline) alignments were performed. Voltage alignment was based on the ECG T-P-interval recognized and displayed as the "true zero," which should always be at baseline and which is used as a reference of S-T segment deviation since there are no specific disease conditions that elevate or depress the T-P segment.

The mathematical formulation is based on a complex linear regression model, which is beyond the scope of this paper, that automatically corrects for any breathing-related baseline shifts or baseline noise. Few sporadic extreme noises were eliminated from the final enhanced graphic formation.

For temporal alignment, the well detectable R wave peak was chosen as a "point of collection" for all the cycles, after baseline alignment.

DISPLAY

We developed a novel method for displaying multiple complexes on a single image. Our method enables rapid observation of both the structure of the complex and the variations as well as outliers that may occur in each ECG lead. After alignment for voltage by baseline correction, and for time by peak R-wave, we superimposed all ECG cycles on top of each other in a 2-R-R interval window. Regions of the image that had a denser collection of beats were brighter and more strongly colored. The bordering red lines represent one standard deviation from the voltage median position [Figure 1, Figure 2, Figure 3, Figure 4]. The R-R interval variability is added as an extra diagnostic tool.

Figure 1. Enhanced lead I versus the traditional standard electrocardiogram (ECG) of a patient with normal ECG and normal coronary arteries. Note on the enhanced lead, the much better graphic display and no voltage spread and the R-R interval variability rate

1: Acquired electrocardiogram (ECG) multiple complexes. **2:** R-R intervals (horizontal axis: minutes, vertical axis: time sampling units: 2000 = 1 second). **[A]** enhanced lead (horizontal axis: time sampling unit: 2000 = 1 second, vertical axis: voltage sampling units). **[B]** Traditional standard lead (corresponding lead). The complete normal standard ECG is depicted to show also the gain and bandwidth

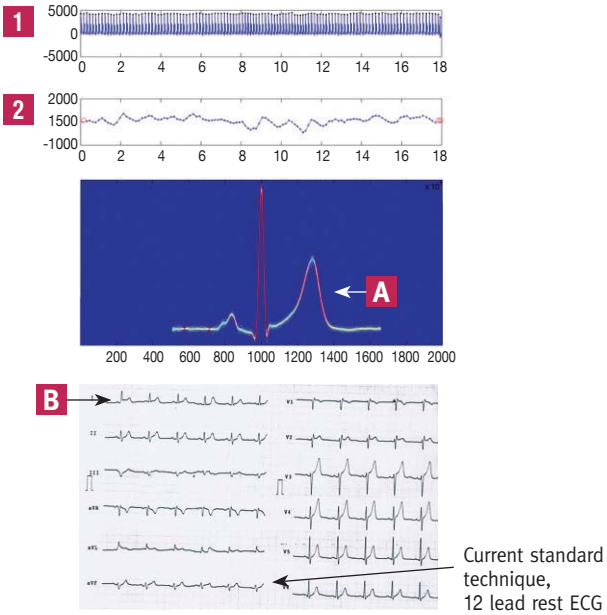

STATISTICAL METHOD

Student's *t*-test was used to calculate *P* values for all variables. To compare between the leads, we used the paired sample test. For prediction analysis we used the receiver operating characteristic (ROC) curves for all leads together and for each lead separately. We used the best area under the curve (AUC) to obtain sensitivity and specificity. Statistical analysis was performed using IBM SPSS statistics software, version 20 (IBM Corp, Armonk, NY, USA).

DIAGNOSTIC ACCURACY STUDY

We studied consecutive patients who were scheduled for a coronary angiogram for standard clinical indications. Exclusion criteria were: clinical instability, multiple premature electrical activity or atrial fibrillation, conduction abnormalities, and refusal to participate in the study.

Prior to performing the coronary angiogram, a standard rest 12-lead ECG recording was obtained from all patients. Clinical data were documented and all ECG recordings were stored digitally for off-line analysis.

Three minute recordings of synchronized multi-leads were acquired (leads I-II-III and leads V2-V4-V6, which are good representations of the limbs and the chest leads).

Figure 2. Enhanced lead I versus the traditional standard lead I of a patient with 3-vessel coronary artery disease. Note on the enhanced lead, the much better graphic display, the S-T-elevation and the extra wave at the J point that cannot be seen in the standard electrocardiogram below. Note also the low R-R interval variability rate

1: Acquired electrocardiogram (ECG) multiple complexes. **2:** R-R intervals (horizontal axis: minutes, vertical axis: time sampling units: 2000 = 1 second). **[A]** enhanced lead (horizontal axis: time sampling unit: 2000 = 1 second, vertical axis: voltage sampling units). **[B]** Traditional standard lead (corresponding lead). The complete normal standard ECG is depicted to show also the gain and bandwidth

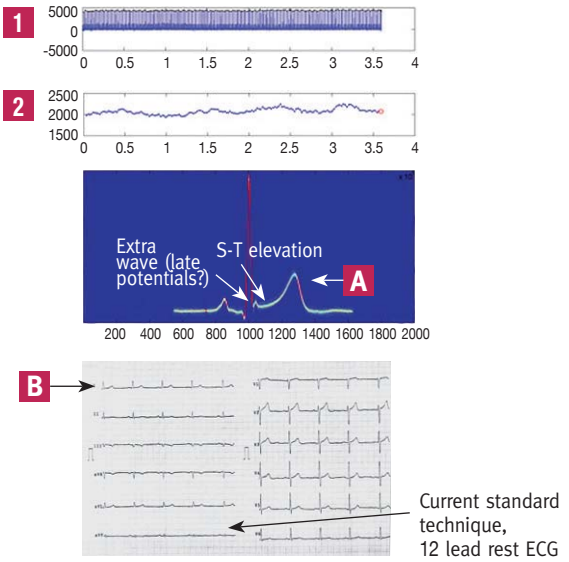

Figure 3. Enhanced lead II versus the traditional standard lead II of a patient with significant left main disease and total right coronary artery occlusion. Note on the enhanced lead, the superior graphic display and the S-T-depression that can be appreciated in the enhanced figure but not in the standard electrocardiogram (ECG) below. Note also the low R-R interval variability rate

1: Acquired electrocardiogram (ECG) multiple complexes. **2:** R-R intervals (horizontal axis: minutes, vertical axis: time sampling units: 2000 = 1 second). **[A]** enhanced lead (horizontal axis: time sampling unit: 2000 = 1 second, vertical axis: voltage sampling units). **[B]** Traditional standard lead (corresponding lead). The complete normal standard ECG is depicted to show also the gain and bandwidth

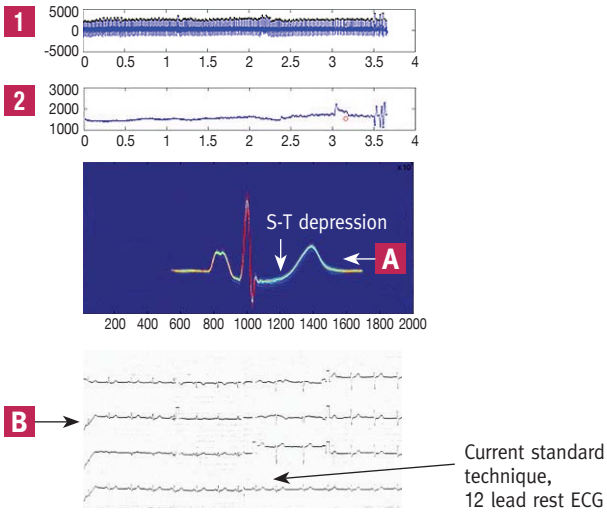

Figure 4. Enhanced lead II of a patient with a normal rest 12-lead electrocardiogram (ECG) but with severe coronary artery disease. Note on the enhanced lead, the typical wide voltage spread. The two red lines bordering the ECG complex represent one standard deviation from the voltage median position. Note also the low R-R interval variability rate

1: Acquired electrocardiogram (ECG) multiple complexes. **2:** R-R intervals (horizontal axis: minutes, vertical axis: time sampling units: 2000 = 1 second). **[A]** enhanced lead (horizontal axis: time sampling unit: 2000 = 1 second, vertical axis: voltage sampling units). **[B]** Traditional standard lead (corresponding lead). The complete normal standard ECG is depicted to show also the gain and bandwidth

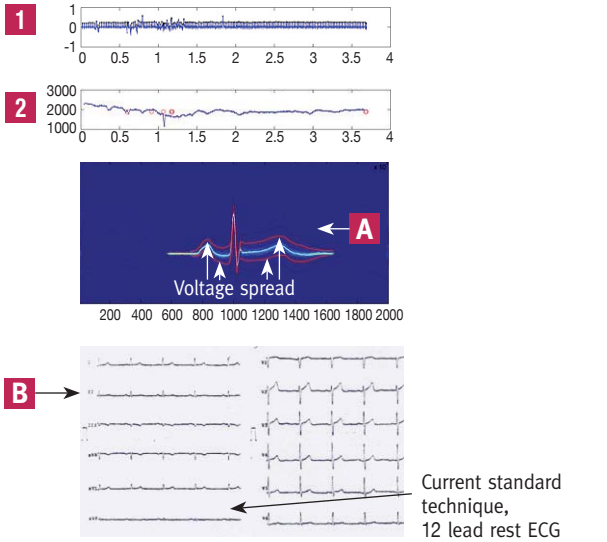

Our gold standard was coronary anatomy obtained by angiography. Patients were classified as having normal coronary arteries (NCA) or significant CAD, which was defined as ≥ 50% stenosis of the minimal lumen diameter in any major coronary artery.

The study protocol was approved by the Hillel Yaffe Medical Center institutional review board and ethics committee. The study was registered as NCT01909817.

RESULTS

We recruited 504 patients for participation in this study. First, to learn the method, we included all comers with no exclusion criteria, and then we focused on patients with normal rest 12-lead ECG. Mean age was 58 ± 12 years, 375 (74%) were males, 135 (27%) presented with acute MI, 53 (11%) with unstable angina, 80 (16%) with chest pain only, 138 (27%) with chest pain and ECG changes, and 98 (19%) with ischemia in a functional test (cardiac stress test, radio-nucleic scan, stress echo).

ECG ENHANCEMENT DISPLAY AND NEW FEATURES

The first aim of this study was to depict the novel graphic capability of the new algorithm. Using our enhancement method, several new ECG graphic features with unique qualities emerged.

The following are selected examples that demonstrate the virtues of the enhanced ECG display:

- **Example 1:** Figure 1 presents an enhanced lead I versus the regular standard ECG of a 45 year old man presenting with chest pain and a normal 12-lead ECG. The angiogram showed NCA. Lead 1, as shown in the standard recording, varies from complex to complex, and thus, a consistent interpretation based on this lead is difficult. In contrast, the same lead I after signal enhancement, has a much better quality and superb visualization of even minute features of the electrical activity, such as the appearance of two atrial components in the P wave, which are not visible in the standard recording. In addition, prominent R-R interval variability can be seen in the top panel.
- **Example 2:** Figure 2 presents an enhanced lead I versus the regular standard lead I of a 76 year old man presenting with anginal pain. His standard 12-lead rest ECG was normal. The angiogram showed triple vessel CAD. Besides

the improved visualization, additional features emerge from the enhanced graphics, which cannot be appreciated on the standard rest-ECG: a mild degree of S-T elevation, a small additional wave following the QRS complex (that may represent late potentials), and poor R-R interval variability on the top panel.

- **Example 3:** Figure 3 presents the enhanced lead II versus the regular standard lead II of a 72 year old woman presenting with congestive heart failure (CHF) and chest pain. Her standard 12-lead rest ECG was normal and not diagnostic of CAD. Her angiogram showed a 70% narrowing of the left main ostium with a catheter-induced pressure drop and total occlusion of a non-dominant right coronary artery (RCA). The enhanced ECG differed from the standard lead in the clearly superior graphical qualities, the appearance of S-T depression that can hardly be seen in the standard lead, a wide, double peaked P wave that emerged, and the demonstration of poor R-R interval variability on the top panel.

VOLTAGE SPREAD: A NEW OBSERVATION THAT MAY CORRELATE WITH CAD

In a subgroup of 152 (30%) patients we observed normal rest 12-lead ECG. Of them, 61 (40%) had significant CAD and 91(60%) had NCA. We noted on the enhanced display, an overall increase in S-T and P-R voltage level variability, mainly in patients with CAD. To quantify these phenomena we measured the width of this voltage spread (VS) at the S-T, the P-R and the T-P intervals, at three similar locations in each interval, on the same ECG lead (beginning, middle, and end), and obtained the mean width of the voltage variance for each interval. This result can be seen in the enhanced graph, in which the width is measured between the two lines, representing one standard deviation from the voltage median position [Figure 4]. To normalize the electrical variance among patients, we first computed the variance at the T-P interval, under the assumption that this variance represents the underlying measurement of noise. We then divided the mean VS at the S-T and P-R intervals by the mean VS at the T-P interval for the same patient in the same lead, and obtained normalized VS values for the S-T and P-R intervals ("VS at S-T" and "VS at P-R", respectively).

Figure 1 shows an example of an enhanced lead I in a patient with NCA and almost no VS. In contrast, Figure 4 shows an example of an enhanced lead II of a patient with severe CAD and wide VS. Both patients had a normal baseline standard ECG.

We analyzed normalized VS in the S-T and the P-R intervals in six leads (I, II, III and V2, V4, V6) for each patient. Mean values of the normalized VS in the S-T interval for the group with CAD versus the group with NCA were 5.61 ± 3.79 vs. 4.01 ± 2.1 ($P < 0.05$). A trend toward a similar phenomenon was noted for the P-R interval (5.37 ± 3.63 in CAD vs. 3.92 ± 2.31 in NCA patients, $P = 0.07$).

Comparing results of VS between CAD and NCA patients, the most significant differences were noted in lead V2 and in patients with two-vessel disease (P values 0.03 and 0.02, respectively). Using the ROC curve method, the largest area under the ROC curve was found for lead V2 (0.719) with a 67% sensitivity and 60% specificity to reveal coronary disease by the normalized VS criteria.

DISCUSSION

In the current study we describe a new method to acquire, enhance, and display rest-ECG signals. For each patient we acquired multiple consecutive ECG cycles at rest with a standard ECG machine (about 200 cycles per lead). The data was processed using a dedicated algorithm developed by BSA (Tel Aviv, Israel), which involved aligning the complexes for time to the R-wave peak, and for voltage to the T-P interval, and then superimposing them to assemble an enhanced display for each lead. This enhanced display presented a superior resolution [Figure 1, Figure 2, Figure 3, Figure 4] compared to standard ECGs, and in our view, brings the long standing 19th century ECG graphic display to the 21st century. It also enabled derivation of new ECG parameters that could distinguish, in patients having normal standard ECG, between those with and without CAD. Remarkably, the normalized VS criteria detected coronary disease with greater sensitivity than was reported in a study of patients with S-T/T abnormalities, 67% vs. 51% [3].

The enhanced ECG signal enables a better visual display and shows details that could not be appreciated on traditional standard ECGs. These features facilitate the reading and interpretation of the standard rest 12-lead -ECG. The new method is more intuitive to the common physician than several systems that claim better ECG visualization and interpretation such as:

- Standardized seventeen segment bull's eye plot [3,4]
- Signal averaged electrocardiography [3,5]
- Derived "3-dimensional" (spatial/spatio-temporal) ECG [6-9]
- High-frequency QRS ECG [10]
- Detailed studies of waveform complexity by singular value decomposition (SVD) [11-13]
- Beat-to beat QT variability (QTV) [14-17]
- R-wave to R-wave variability (RRV) [18-20]

Most of these systems share a common problem: they display specific graphics that are not yet established in the general medical practice and are not familiar to most clinicians. Our display method merely enhances the visualization of the classic ECG waveforms, enabling clinicians to interpret the ECG with only minutes of training, while at the same time making it substantially easier to locate anomalies in the ECG.

Our system uses signal summation, which is totally different from the signal averaged electrocardiography (SAECG) method [5]. SAECG uses temporal averaging to reduce "random" or "uncorrelated noise" by calculating the square root of the number of waveforms averaged, in an attempt to resolve detailed features on the ECG complex. The described enhancement is not the result of simple "zooming-in", because each added cycle (all together around 200) augments the graphic display of the specific lead.

As we have shown, in patients with normal rest 12-lead ECGs but who had CAD, we observed a random cycle-to-cycle shift of the baseline voltage, mainly at the S-T interval, and to a lesser extent at the P-R interval. This VS phenomenon could be seen only after voltage alignment to the T-P interval, as described previously. The superimposition with summation of multiple cycles is a unique feature of our new method. As shown, VS was significantly more prevalent in patients with CAD than in those with NCA (for example, Figure 1 for NCA vs. Figure 4 for CAD). Thus, VS cannot be explained by changes in heart rate or respiratory motion, as our improved baseline depends only on the T-P intervals before and after each cycle, as explained in the Patients and Methods section. In this study, we have shown that this newly described phenomenon correlates with CAD and can thus increase the diagnostic power of standard rest ECG recordings. We did not study the correlation between VS and other heart diseases and we included only patients with known coronary anatomy acquired by angiogram.

The VS is an observational phenomenon unique to our system and is described for the first time. It may have several theoretical explanations that require further scientific validation. It can be explained by uneven propagation of the cardiac electrical activity in hearts with some degree of atherosclerosis. This phenomenon can be seen mainly at the S-T interval, which represents the energy requiring re-polarization phase of the heart action potential, mainly at the left ventricle level. Similar phenomena can be seen, to a lesser degree, at the P-R interval, which represents the atria re-polarization. Relative or regional ischemia may induce spatially discordant alternans [21]. As a result, the action potential duration may alternate out of phase in different regions of the heart, markedly enhancing dispersion of refractoriness.

LIMITATIONS

Our novel observations regarding the "voltage spread" phenomenon are preliminary results that need further studies and validation on a larger patient group. Future studies should also address the relationship between CAD and R-R interval variability, as obtained by this new method. The added value of the enhanced ECG to other cardiologic disorders (arrhythmias, conduction disturbances, cardiomyopathies) has yet to be explored.

CONCLUSIONS

We describe a new technology that enhances and improves standard ECG display, and which may markedly increase clinicians' ability to analyze and interpret ECG. The enhanced ECG display may increase the diagnostic value of rest ECGs to detect CAD by using the familiar, inexpensive, easy-to-perform and side-effect-free, standard rest-ECG while retaining its well-known format. Further validation following recruitment of a larger group of patients in a multi-center study, is still needed.

Correspondence
Dr. A. Frimerman
Head, Dept. of Cardiology, Hillel Yaffe Medical Center, Hadera 38100 Israel
Fax: (972-4) 618-8369
email: afrimer@gmail.com

References

1. Einthoven W. Galvanometrische registratie van het menschilijk electrocardiogram. In: Rosenstein SS, ed. Herinneringsbundel Leiden: *Eduard Ijdo*, 1902: 101-107.
2. Pirwitz MJ, Lange RA, Landau C, MeShack BM, Hillis LD, Willard JE. Utility of the 12-lead electrocardiogram in identifying underlying coronary artery disease in patients with depressed left ventricular systolic function. *Am J Cardiol* 1996; 77: 1289-92.
3. Mahmoodzadeh S, Moazenzadeh M, Rashidinejad H, Sheikhvatan M. Diagnostic performance of electrocardiography in the assessment of significant coronary artery disease and its anatomical size in comparison with coronary angiography. *J Res Med Sci* 2011; 16: 750-5.
4. Gregg RE, Helfenbein DE, Zhou SH. Graphic visualization of ECG estimated myocardial infarct size using the standardized seventeen segment bull's eye plot. *Comput Cardiol* 2010; 37: 33-6.
5. Lee KL, Lau CP. The use of signal-averaged electrocardiogram in risk stratification after acute myocardial infarction in the modern era. *Eur Heart J* 2005; 26: 747-8.
6. Kardys I, Kors JA, van der Meer IM, Hofman A, van der Kuip DA, Witteman JC. Spatial QRS-T angle predicts cardiac death in a general population. *Eur Heart J* 2003; 24: 1357-64.
7. Fayn J, Rubel P, Pahlm O, Wagner GS. Improvement of the detection of myocardial ischemia thanks to information technologies. *Int J Cardiol* 2007; 120: 172-80.
8. Rautaharju PM, Kooperberg C, Larson JC, LaCroix A. Electrocardiographic predictors of incident congestive heart failure and all-cause mortality in postmenopausal women: the Women's Health Initiative. *Circulation* 2006; 113: 481-9.
9. Yamazaki T, Froelicher VF, Myers J, Chun S, Wang P. Spatial QRS-T angle predicts cardiac death in a clinical population. *Heart Rhythm* 2005; 2: 73-8.
10. Schlegel TT, Kulecz WB, DePalma JL, et al. Real-time 12-lead high frequency QRS electrocardiography for enhanced detection of myocardial ischemia and coronary artery disease. *Mayo Clin Proc* 2004; 79: 339-50.
11. Okin PM, Malik M, Hnatkova K, et al. Repolarization abnormality for prediction of all-cause and cardiovascular mortality in American Indians: the Strong Heart Study. *J Cardiovasc Electrophysiol* 2005; 16: 945-51.
12. Zabel M, Malik M, Hnatkova K, et al. Analysis of T-wave morphology from the 12-lead electrocardiogram for prediction of long-term prognosis in male US veterans. *Circulation* 2002; 105: 1066-70.
13. Batdorf BH, Feiveson AH, Schlegel TT. The effect of signal averaging on the reproducibility and reliability of measures of T-wave morphology. *J Electrocardiol* 2006; 39: 266-70.
14. Berger RD, Kasper EK, Baughman KL, Marban E, Calkins H, Tomaselli GF. Beat-to-beat QT interval variability: novel evidence for repolarization lability in ischemic and nonischemic dilated cardiomyopathy. *Circulation* 1997; 96: 1557-65.
15. Piccirillo G, Magri D, Matera S, et al. QT variability strongly predicts sudden cardiac death in asymptomatic subjects with mild or moderate left ventricular systolic dysfunction: a prospective study. *Eur Heart J* 2007; 28: 1344-50.

16. Vrtovec B, Sinkovec M, Starc V, Radovancevic B, Schlegel TT. Coronary artery disease alters ventricular repolarization dynamics in type 2 diabetes. *Pacing Clin Electrophysiol* 2005; 28: S178-81.

17. Starc V, Schlegel TT. Real-time multichannel system for beat-to-beat QT interval variability. *J Electrocardiol* 2006; 39: 358-67.

18. Camm AJ, Malik M, Bigger JT Jr, et al. Heart rate variability. Standards of measurement, physiological interpretation, and clinical use. Task Force of the European Society of Cardiology and the North American Society of Pacing and Electrophysiology. *Eur Heart J* 1996; 17: 354-81.

19. Goldberger AL, Amaral LA, Hausdorff JM, Ivanov P, Peng CK, Stanley HE. Fractal dynamics in physiology: alterations with disease and aging. *Proc Natl Acad Sci USA* 2002; 99: 2466-72.

20. Schlegel TT, Kulecz WB, Feiveson AH, et al. Accuracy of advanced versus strictly conventional 12-lead ECG for detection and screening of coronary artery disease, left ventricular hypertrophy and left ventricular systolic dysfunction. *BMC Cardiovasc Disord* 2010; 10: 28.

21. Garfinkel A. Eight (or more) kinds of alternans. *J Electrocardiol* 2007; 40: S70-74

Capsule

Why aging attenuates antiviral responses

Older adults are more likely to die after influenza A viral infection than younger adults. This effect is in part because monocytes from older people produce less interferon and show reduced induction of antiviral genes in response to infection. **Molony** and co-authors found that monocytes from older human donors showed impaired signaling downstream of the cytosolic RNA sensor RIG-I, which initiates the innate immune response to influenza A virus. Thus, restoring RIG-I signaling in older individuals may reduce age-related mortality from influenza A viral infection.

Sci Signal 2017; 10: eaan2392

Eitan Israeli

Capsule

Asprosin is a centrally acting orexigenic hormone

Asprosin is a recently discovered fasting-induced hormone that promotes hepatic glucose production. **Duerrzchnid** and colleagues demonstrated that asprosin in the circulation crosses the blood–brain barrier and directly activates orexigenic AgRP+ neurons via a cAMP-dependent pathway. This signaling results in inhibition of downstream anorexigenic proopiomelanocortin (POMC)-positive neurons in a GABA-dependent manner, which then leads to appetite stimulation and a drive to accumulate adiposity and body weight. In humans, a genetic deficiency in asprosin causes a syndrome characterized by low appetite and extreme leanness. This phenomenon is phenocopied by mice carrying similar mutations and can be fully rescued by asprosin. Furthermore, the authors found that obese humans and mice had pathologically elevated concentrations of circulating asprosin and neutralization of asprosin in the blood with a monoclonal antibody reduced appetite and body weight in obese mice, in addition to improving their glycemic profile. Thus, in addition to performing a glucogenic function, asprosin is a centrally acting orexigenic hormone that is a potential therapeutic target in the treatment of both obesity and diabetes.

Nature Med 2017; 23: 1444

Eitan Israeli

Capsule

Incidence of hip and knee replacements in patients with rheumatoid arthritis following the introduction of biological DMARDs

Lindholm Cordtz et al. studied the impact of the introduction of biological disease-modifying anti-rheumatic drugs (bDMARDs) and associated rheumatoid arthritis (RA) management guidelines on the incidence of total hip replacement (THR) and total knee replacement (TKR) in Denmark. The authors identified 30,404 patients with incident RA and 297,916 general population cases (GPCs). In 1996, the incidence rate of THR and TKR was 8.72 and 5.87, respectively, among patients with RA, and 2.89 and 0.42 in GPCs. From 1996 to 2016, the incidence rate of THR decreased among patients with RA, but increased among GPCs. Among patients with RA, the incidence rate of TKR increased from 1996 to 2001, but started to decrease from 2003 and throughout the bDMARD era. The incidence of TKR increased among GPCs from 1996 to 2016. The authors concluded that the incidence rate of THR and TKR was threefold and 14-fold higher, respectively, among patients with RA compared with GPCs in 1996. In patients with RA, introduction of bDMARDs was associated with a decreasing incidence rate of TKR, whereas the incidence of THR had started to decrease before bDMARD introduction.

Ann Rheum Dis 2017; annrheumdis-2017-212424

Eitan Israeli